Simulation of Oil-Water Core-Annular Flow through an Inclined Pipe

Master thesis
Submitted on
at

POLITECNICO DI MILANO

For the master's degree in Energy Engineering

By
Ehsan Yaghoubi

Student ID: 926872
Academic year: 2021-2022

Supervisors:

Professor Riccardo Mereu (POLIMI) main supervisor
Professor Luigi Pietro Maria Colombo, (POLIMI) co-supervisor

POLITECNICO
MILANO 1863

تقدیم به روح پاک مادرم

تقدیم به پدرم

که تمام هستی ام از آن دوست

To my beloved mom and dad
Far from my sight
But always in my heart

Abstract

The present work reports a Volume of Fluid (VOF) multiphase flow simulation of oil-water core-annular flow through an inclined pipe (15° downward inclination angle with respect to the horizontal). Three different geometries of the flow entry and initial mixing region (i.e., nozzle part) have been sketched for the simulations: (1) a “simplified” geometry, in which water and oil are injected and mixed at the inlet section of the main pipe without any nozzle part; (2) a “branch” geometry, in which water and oil are injected through a branch then mixed in the nozzle, (3) an “extended” geometry, in which water and oil are injected through an extended pipe then mixed in the nozzle. A structured hexahedral grid has been created for each geometry. In all the cases, water is injected circumferentially, whereas oil is injected annularly [19].

Simulated results with respect to each geometry were compared with experimental results [25]. The simulations were run for 8 flow conditions with oil superficial velocity ranging from 0.56 to 1.06 [m/s] and with water superficial velocity ranging from 0.66 to 1.33 [m/s]. The turbulence models realizable k-ε and Transition SST are set for steady state pseudo-transient simulations [24] . The “extended” geometry shows the trend closest to the experimental results. The average oil holdup obtained from simulations is consistent with the experimental data with a maximum deviation error.

Keywords:

Simulation, The volume of Fluid (VOF), Oil-Water, core annular, multiphase flow

Sommario

Il presente lavoro riporta una simulazione di flusso multifase a volume di fluido (VOF) di un flusso di olio e acqua attraverso un tubo inclinato (angolo di inclinazione di 15° rispetto all'orizzontale). Per le simulazioni sono state disegnate tre diverse geometrie dell'ingresso del flusso e della regione di miscelazione iniziale (cioè la parte dell'ugello): (1) una geometria "semplificata", in cui l'acqua e l'olio vengono iniettati e miscelati all'ingresso del tubo principale senza alcuna parte dell'ugello; (2) una geometria "ramificata", in cui l'acqua e l'olio vengono iniettati attraverso una diramazione e poi miscelati nell'ugello; (3) una geometria "estesa", in cui l'acqua e l'olio vengono iniettati attraverso un tubo esteso e poi miscelati nell'ugello. Per ogni geometria è stata creata una griglia esaedrica strutturata. In tutti i casi, l'acqua viene iniettata circonferenzialmente, mentre l'olio viene iniettato anularmente [19]

I risultati simulati per ciascuna geometria sono stati confrontati con i risultati sperimentali [25]. Le simulazioni sono state eseguite per 8 condizioni di flusso con velocità superficiale dell'olio compresa tra 0,56 e 1,06 [m/s] e con velocità superficiale dell'acqua compresa tra 0,66 e 1,33 [m/s]. I modelli di turbolenza realizzabili k-ε e Transition SST sono impostati per simulazioni pseudo-transienti allo stato stazionario [24] . La geometria "estesa" mostra l'andamento più vicino ai risultati sperimentali. La portata media dell'olio e la caduta di pressione ottenute dalle simulazioni sono coerenti con i dati sperimentali con un errore di deviazione massimo.

Parole chiave:

simulazione; il volume del fluido (VOF); olio-acqua; nucleo anulare; flusso multifase

Acknowledgments

I would like to thank my supervisors professor Colombo professor Mereu, ing. Passoni and ing. Carraretto for introducing me with this interesting topic. I owe them a debt of gratitude for their precious support during the project. I am honored to have had the opportunity to work with them.

I want to thank my friends in Italy, for all your help, support and encouragement.

I want to thank my family whom I miss. For your constant support, your encouragement, and your love. I am thankful for having you in my life, and for every single moment that I spent with you which is precious to me.

Contents

Nomenclature

Abbreviations

VOF	Volume of Fluid
SRQ	System Response Quantity
RD	Relative Deviation
MRD	Mean Relative Deviation
MARD	Mean Absolute Relative Deviation
u	x-velocity
v	y-velocity
t	time
p	pressure
Re	Reynolds number

λ	
H	Hold-up
μ	viscosity
Ω	Boundary Condition
D	Diffusivity
ρ	Density
η	
δ	
Q	Flow Rate
RD	Relative Deviation
τs	
f	Fanning friction factor
J	The mixture of superficial velocity

1
Introduction

1.2. OBJECTIVES OF THE STUDY

The present work aims to contribute on characterizing the oil-water core annular downflow inside inclined pipes. Several previous works are available in open literature with regards to oil-water core annular flow, mostly physical experiments. The present thesis work instead reports a Volume of Fluid (VOF) multiphase flow simulation of oil-water core-annular flow inside an inclined pipe.

Since 2003, several experimental set-ups have been built in the Single and Multiphase Thermal Fluid Dynamics Laboratory at the Energy Department of Polytechnic di Milano to characterize different regimes of oil-water flow. The set-ups were either horizontal or mainly low slope, from 1.5 degrees downward up to 6 degrees upward [2]. Most recently in 2021, Franchi built a piping set-up with 15 degrees of inclination to analyze the behavior of oil-water core annular flow experimentally [1]. The present work is a follow-up numerical research based on Franchi's experiments.

It is a common practice in all engineering and scientific fields to calibrate a computational model based on physical experiments. The computational model is "validated" if the computational results agree with experimental data. Subsequently, the present thesis work attempts to calibrate the VOF model in ANSYS Fluent and validate Franchi's main experimental results.

Consequently, the main objectives of this work are categorized as follows:

- Building up a suitable geometry and mesh for the simulations based on the experimental set-up
- Developing the base set-up in ANSYS Fluent to proceed with the main simulations

- Numerically determining the flow patterns and post-processing the main results e.g., oil/water hold-up and distributed pressure drop
- Comparing the simulation results of phase hold-up and distributed pressure drop with the experimental data
- Deriving the wall friction factor

1.3. THESIS OUTLINE

The current thesis work contains five chapters:

- Chapter 1: introduces the motivation behind the research work, the hypothesis assumed, and the main objectives achieved throughout conducting the project.
- Chapter 2: provides a literature review on oil-water core annular flow and the background of the work
- Chapter 3: describes the methodology adopted in ANSYS (geometry, mesh, set-up, and solution)
- Chapter 4: contains postprocessing of the results (flow patterns, oil holdup, pressure drop)
- Chapter 5: presents the conclusion of the study and recommendations for future works

2
Background

The aim of this chapter is to provide a brief literature review on the subject and the background of the problem.

2.1. NUMERICAL WORKS

In 2002, Gao et al [16] numerically simulated the stratified oil-water two phase turbulent flow in a horizontal tube using a volume of fluid model. They applied the RNG k–e model combined with a near-wall low-Re turbulence model. They adopted a continuum surface force approximation for the calculation of surface tension. In 2019, Santos et al. [21] investigated the stratified flow of a mixture of paraffin oil water with different concentrations of the oil phase both experimentally and numerically. Their simulations were conducted in COMSOL Multiphysics mainly in 2D implementing the $k - \varepsilon$ turbulence model. In 2020, Dewangan et al [20] conducted the simulation of stratified oil-water flow in a 2D channel on ANSYS Fluent. They investigated the effect of various parameters such as density ratio, kinematic viscosity and surface tension coefficient on the mixture velocity and total pressure change. In 2021, Bochio et al [19] studied stratified viscous oil water flow both experimentally and numerically in OpenFOAM. They showed significant differences between Reynolds Average Navier-Stokes and large eddy simulations for turbulence in this case study.

2.2. OUTLET BC

Mathematical modeling of fluid flow problems often deals with unbounded domains. To reduce the computational cost while simulating fluid flow in an unbounded

domain, one strategy would be to truncate the domain of interest and define an artificial boundary condition. In literature, this type of artificial boundary condition approximates the so-called “transparent" boundary condition (i.e., such that the solution of the problem in the bounded domain is equal to the solution in the original domain). The transparent boundary condition for a time dependent case is defined as an integral relation in time and space between the velocity and its normal derivative on the boundary [23] .

In 1993, Jin and Braza [15] developed a nonreflecting boundary condition for the full incompressible unsteady Navier Stokes equation.

$$u_t + uu_x - \frac{1}{Re}u_{yy} = 0 \quad and \quad v_t + uv_x - \frac{1}{Re}v_{yy} = 0 \tag{1}$$

In 1989, Halpern and Schatzman [8] designed a convective boundary condition

$$u_t + U.\nabla u = 0 \quad and \quad v_x = 0 \tag{2}$$

where $U(x,t) = (U(x,t), V(x,t))$ is a known flow. This U function can be a ‘typical’ known homogenous flow.

In 2000, Ol’shanskii and Staroverov [12] proposed a simple convective boundary condition called the *drift condition*:

$$\frac{\partial \boldsymbol{u}}{\partial t} + \boldsymbol{U}\frac{\partial \boldsymbol{u}}{\partial n} = 0, \quad \boldsymbol{u} = (u, v) \tag{3}$$

Where $U(x)$ called the *drift function* is formally chosen as either of the options below:

$$\boldsymbol{U}(x) = (U_{constant}, 0) \quad or \quad \boldsymbol{U}(x) = (P(y), 0) \tag{4}$$

Where $P(y)$ is the Poiseuille profile.

Only for stationary solution, they obtained $v = 0$ for the outlet BC. In this case, the conditions of Halpern-Schatzman coincide with Ol’shanskii and Staroverov.

If the outflow is unknown and unsteady state, U can be computed through the following formulations:

$$U = \frac{\int_{\partial\Omega_{out}} u_t \, dy}{\int_{\partial\Omega_{out}} u_x \, dy} = \frac{\left(\int_{\partial\Omega_{out}} u \, dy\right)_t}{\int_{\partial\Omega_{out}} u_x \, dy} \tag{5}$$

Since mass flux is balanced $\int_{\partial\Omega_{in}} u \, dy = \int_{\partial\Omega_{out}} u \, dy$,

$$U = \frac{\left(\int_{\partial\Omega_{in}} u\, dy\right)_t}{\int_{\partial\Omega_{out}} u_x\, dy} \tag{6}$$

In 2016, Li et al [22] proposed a simple and efficient transparent boundary condition to simulate channel-type flows. They utilized a weak formulation to simulate fluid flow at low Reynolds number.

$$u_t + uu_x = 0 \quad and \quad v = 0 \tag{7}$$

To avoid suffering from numerical difficulties, they reformed the formulation using the divergence-free condition $\nabla . u = 0$

$$u_t + uu_x = u_t + uu_x + u\left(u_x + u_y\right) = u_t + (u^2)_x = 0 \quad and \quad v = 0 \tag{8}$$

They directly derived the equivalent pressure boundary condition, taking the inner product of Navier-Stokes equation:

$$\boldsymbol{n}.\nabla p = \boldsymbol{n}.\left(-\boldsymbol{u}_t - \boldsymbol{u}.\nabla\boldsymbol{u} + \frac{1}{Re}\Delta\boldsymbol{u}\right) \tag{9}$$

Substituting eq 7 into eq 9

$$p_x = \frac{1}{Re}(u_{xx} + u_{yy}) \tag{10}$$

At high Reynolds numbers, to reduce numerical errors, the method proposed by Li et al [22] requires a large computational domain to reduce numerical errors. In case of multiphase flows, mass conservation should be satisfied for each fluid separately if the mass flux is to be conserved. Therefore, the inflow and outflow should be coupled with the phases in this case.

Studies on multiphase outflow boundary conditions are quite scarce in comparison to single phase. In 2001, Son [9] presented a numerical method for computing unsteady incompressible two-phase flow with open or periodic boundaries based on a level set technique. In 2013, Lou et al [13] investigated the performance of three types of outflow boundary conditions i.e., the Neumann BC, the convective BC, and the extrapolation BC for two phase lattice-Boltzmann equations. In 2014, Dong et al [17] have presented a set of outflow boundary conditions, and an associated numerical algorithm, within the phase-field framework for simulating incompressible two-phase flows involving outflow or open boundaries. The method developed by Dong et el. [17] provides an effective and efficient technique for simulating a large class of crucial two-phase flows, i.e., two-phase jets, wakes, shear layers, and other spatially developing two-phase flows involving inflow/outflow boundaries.

In 2014, Dong et al. [17] presented a method that can maximize the domain truncation without adversely affecting the flow physics. They presented the following boundary condition.

For the velocity

$$-p\boldsymbol{n} + \mu\boldsymbol{n}.\boldsymbol{D}(\boldsymbol{u}) - \left[\frac{\lambda}{2}\nabla\emptyset.\nabla\emptyset + \lambda F(\emptyset)\right]\boldsymbol{n} - \left[\frac{1}{2}\rho|\boldsymbol{u}|^2\Theta_0(\boldsymbol{n}.\boldsymbol{u})\right]\boldsymbol{n} = \boldsymbol{0} \quad on\ \partial\Omega_o \tag{11}$$

For the phase field function:

$$\boldsymbol{n}.\nabla[\nabla^2\emptyset - h(\emptyset)] = 0 \quad on\ \partial\Omega_o \tag{12}$$

$$\boldsymbol{n}.\nabla\emptyset = -D_0\frac{\partial\emptyset}{\partial t} \quad on\ \partial\Omega_o \tag{13}$$

Where $\boldsymbol{D}(\boldsymbol{u}) = \nabla(\boldsymbol{u}) + \nabla(\boldsymbol{u})^T$ and $-1 \le \emptyset \le 1$ is the phase field function. $\emptyset = 1\ and\ \emptyset = -1$ represents the first and the second fluids respectively. The iso-surface corresponds with $\emptyset(x,t) = 0$, the interface between the two fluids at time t is $h(\emptyset) = \frac{1}{\eta^2}\emptyset(\emptyset^2 - 1)$

n is the outward-pointing unit vector normal to $\partial\Omega_o$, $\mu\ and\ \rho$ are respectively the mixture dynamic viscosity and density given as

$$\rho(\emptyset) = \frac{\rho_1 + \rho_2}{2} + \frac{\rho_1 - \rho_2}{2}\emptyset \tag{14}$$

$$\mu(\emptyset) = \frac{\mu_1 + \mu_2}{2} + \frac{\mu_1 - \mu_2}{2}\emptyset \tag{15}$$

And

$$F(\emptyset) = \frac{1}{4\eta^2}(\emptyset^2 - 1)^2 \tag{16}$$

$$\Theta_0(\boldsymbol{n}.\boldsymbol{u}) = \frac{1}{2}(1 - \tanh\left(\frac{\boldsymbol{n}.\boldsymbol{u}}{U_0\delta}\right) \tag{17}$$

where U_0 is a characteristic velocity scale, and $\delta > 0$ is a chosen non-dimensional constant that is sufficiently small. $D_0 \ge 0$ is a chosen non-negative constant and will be referred to as the outflow dynamic mobility.

2.3. SUMMARY AND PROBLEM STATEMENT

Franchi [1] performed an experiment on oil-water multiphase flow in a 15-degree inclination pipe in the Single and Multiphase Thermal-Fluid Dynamics Laboratory at the Energy Department of Polytechnic di Milano. He experimented the core annular regime for sixteen inlet configurations. He measured the frictional pressure gradients and oil hold-up for all the sixteen cases. His results were in good agreement with the mechanistic and empirical models. Figure 1 represents the geometry of the fluid injector attached to the 10-m-long tube of 40 mm diameter. Although, to reduce the computational cost, the geometry of the simulation case is cut to 3 m long.

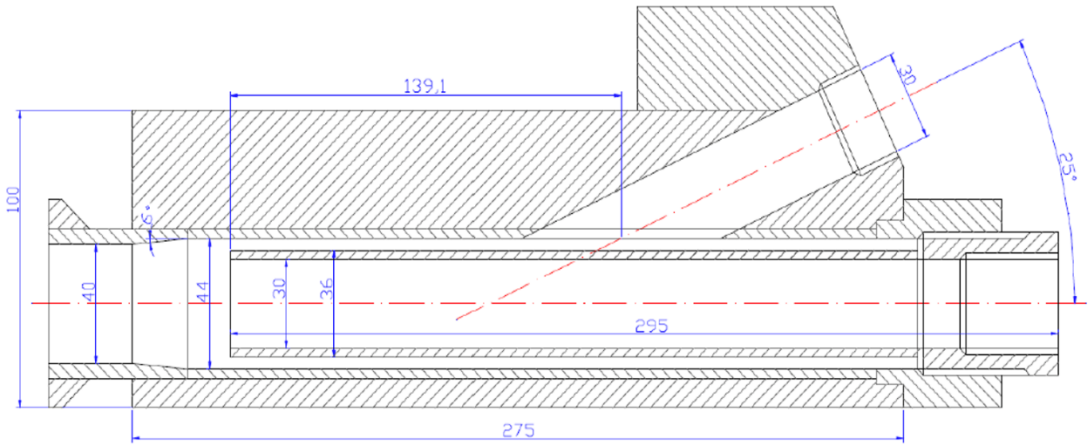

Figure 1 The geometry of the injector, sizes are in millimeters, sketch taken from [1]

Table 1 represents eight of the mentioned sixteen inlet flow rate cases experimented. The problem to address here is the verification of experimental results through computational fluid dynamics simulations in ANSYS Fluent Software.

Table 1 Details of the eight inlet flow rate configurations taken from [1]

Cases	**Oil Flow Rate**	**Water Flow Rate**	**Oil Holdup**	**Pressure Gradient**	
	Q_O	Q_W	H_O [-]	**(dp/dz)T** [kPa/m]	**(dp/dz)F** [kPa/m]
A1	2.52	3.00	0.35	-0.468	-0.374
A4	2.52	6.00	0.23	-0.872	-0.809
B1	3.23	3.00	0.41	-0.632	-0.520
B4	3.23	6.00	0.28	-1.076	-0.999
C1	4.12	3.00	0.46	-0.785	-0.658
C4	4.12	6.00	0.30	-1.251	-1.167
D1	4.79	3.00	0.50	-0.949	-0.812
D4	4.79	6.00	0.35	-1.346	-1.250

3 Methodology

3.1. GEOMETRY AND MESH

3.1.1 'Simple' Case

Figure 2 (a) and (b) shows the schematic of the mesh for simple geometry in front and isometric views respectively. Three levels of mesh (300K, 500K and 1M) were taken under consideration.

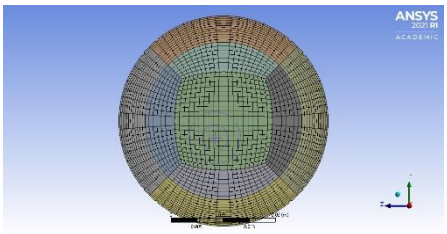

(a) Front view

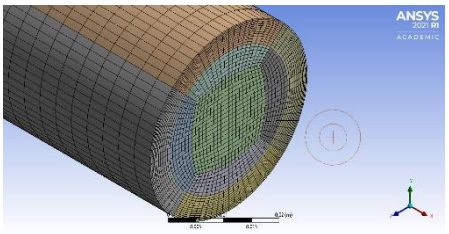

(b) Isometric view

Figure 2 Snapshots of simple geometry

3.1.2 'Branch' Case

Figure 3 (a), (b), and (c) shows the schematic of the mesh for the branch geometry attached to the simple geometry (see (d)) in different views (front, isometric, and side) respectively. The branch mesh contains 1M number of unstructured elements and the simple mesh contains 500K number of structured elements.

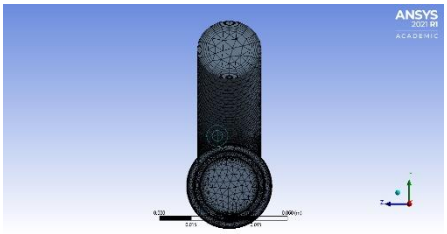

(a) Front view

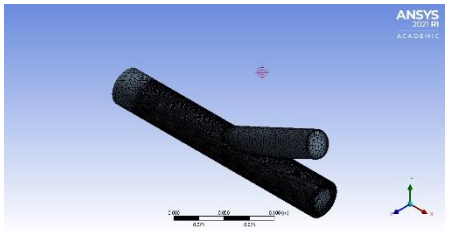

(b) Isometric view

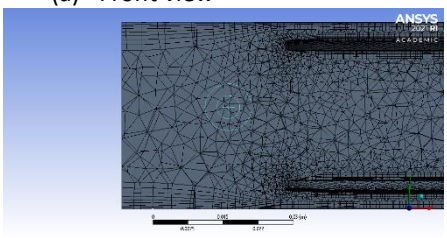

(c) Side view, a cross-section of branch outlet

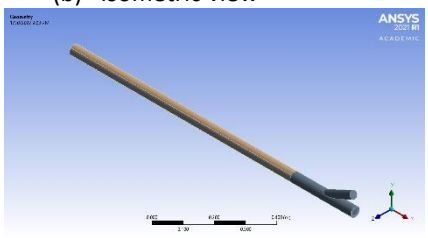

(d) Isometric view of geometry

Figure 3 Schematic of the branch mesh

3.1.3. 'Extended' Case

Figure 5 shows the schematic of the mesh for the extended geometry.

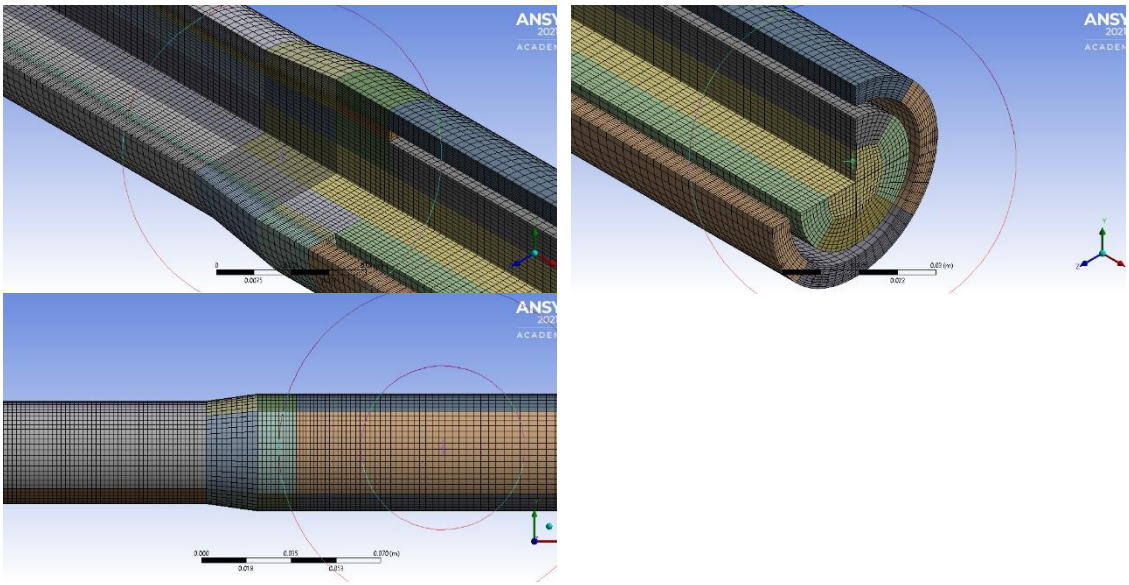

Figure 4 Schematic of the extended geometry and mesh

The mesh is further refined near the wall to reach Yplus values lower than 10. The cross-section and side views of the mesh are then sketched along the length of the tube. The mesh is further adapted at the VOF interface. The refinement control sets 2 levels of refinement, minimum cell volume of 1e-10 m^3, and minimum cell orthogonal quality of 0.01. Table 2 presents details of the adapted grid size of the extended geometry. The final adapted mesh results in a +2M number of added elements in comparison to the non-adapted version.

Table 2 Details of adapted grid size of the extended geometry

	Original	**Adapted**	**Change**
Number of elements	857,895	2,878,172	+2,020,277

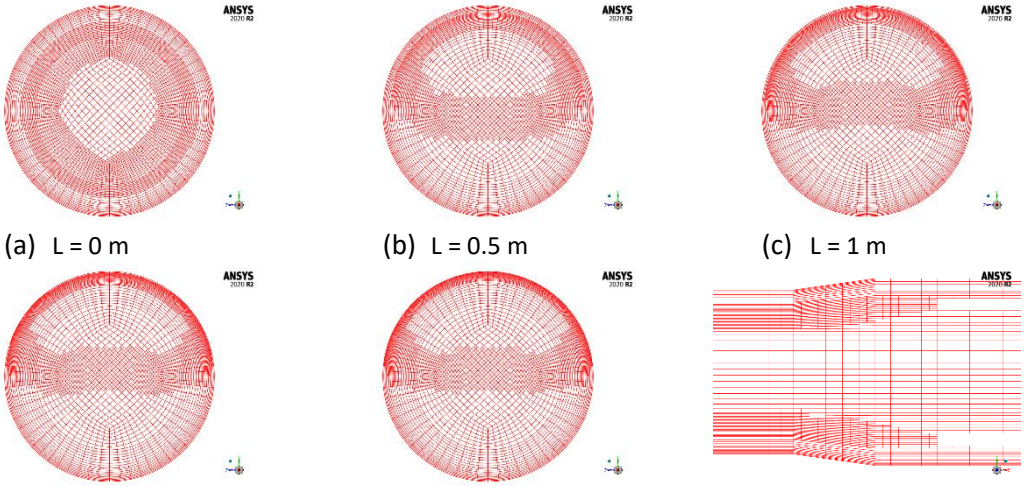

(a) L = 0 m (b) L = 0.5 m (c) L = 1 m

(d) L = 2 m (e) L = 3 m (f) Side view

Figure 5 Schematic of the adaptive mesh refinement (extended version) mesh grid along the tube length

3.3. SET-UP

One of the main tasks to achieve the objective of the study is to assess the use Volume of Fluid (VOF) multiphase flow model in ANSYS Fluent 2020 R2. To do so, the implicit formulation based on the "Compression" scheme of volume of fraction is utilized to capture the interface. This scheme is consistent with the steady state condition. When the aim is to capture the steady state solution and not the intermediate transient flow behavior [7]. The interfacial anti diffusion sharpens the interface [6] and helps capturing the turbulence effects. Gravity force is active with respect to the 15-degree inclination angle. The governing equations are discretized using the finite volume technique. The simulation has been run for pseudo-transient condition, meaning that transient terms have been retained in the formulation. This serves two purposes. Firstly, it has helped in investigating the initial development of core annular flow. Secondly, if there is any temporal variation of the flow phenomena inside the tube, it could be captured through a transient formulation. The simulation is based on the assumptions of immiscible liquid pair, constant liquid properties.

The full details of the simulation settings are provided in the following table. In the case of oil-water core flow, the flow of the oil core is always laminar owing to its very high viscosity while the flow of water in the annular film is turbulent. Since in VOF modeling, both the phase share a common momentum equation, there is no scope to use separate viscous models for both the phases. Therefore, the realizable k–ε and Transition SST have has been used. In this model, the turbulent kinetic energy and viscous dissipation rates are calculated and used to obtain the turbulent viscosity in the flow field.

Table 3 Details of the simulation set-up

Solver	ANSYS Fluent 2020 R2		**Spatial Discretization**	Gradient	Least Squared Cell Based
Time	Pseudo Transient		**Pressure**	Presto!	
Gravity	Active		**Volume Fraction**	Compression	
Multiphase Model	Volume of Fluid (VOF)		**Other**	2nd order upwind	
Viscous Model	k-eps realizable / Transition SST				
P-V Coupling	Coupled				

3.4. BOUNDARY CONDITIONS & INITIALIZATION

ANSYS Fluent provides a finite volume discretization over the Navier-Stokes equations. The main boundary conditions to address the case would simply be as follows:

- Pressure outlet
- Velocity inlet or mass flow rate inlet
- Walls

In the experiment, first, the water stream flows into the tube, and then after some time the oil stream pump starts functioning. Water inlet BC sets the initial values of the field variables in the whole domain.

4
Results

This chapter contains the results of the simulation followed by a discussion regarding the major findings of the analysis.

4.1. GEOMETRY SELECTION

This subsection aims to assess the most efficient geometry to proceed with the simulation. Three different geometries are investigated: the ‘extended’, ‘simple’, and ‘branch’. The simulations are run for the horizontal case in each geometry and the results are compared with the experiment in 8 different oil inlet flow rate cases.

Figure 6 shows the simulation and the experimental trend for oil hold-up versus oil inlet flow rate fraction ε_O in the horizontal case. The simulations show that oil hold-up should increase almost linearly to the oil inlet flow rate fraction. For the minimum superficial velocity, the experimental data deviate from the linear trend for oil flow rate volume fractions above 0.5. This deviation is not observed in the simulation data.

The inconsistency between the simulation and experimental trend of oil holdup is observed for cases C1 and D1. These two cases have almost the same water superficial velocities, but different oil superficial velocities. For these two cases, the simulations estimate different values of oil holdup, while the experiments show the same values.

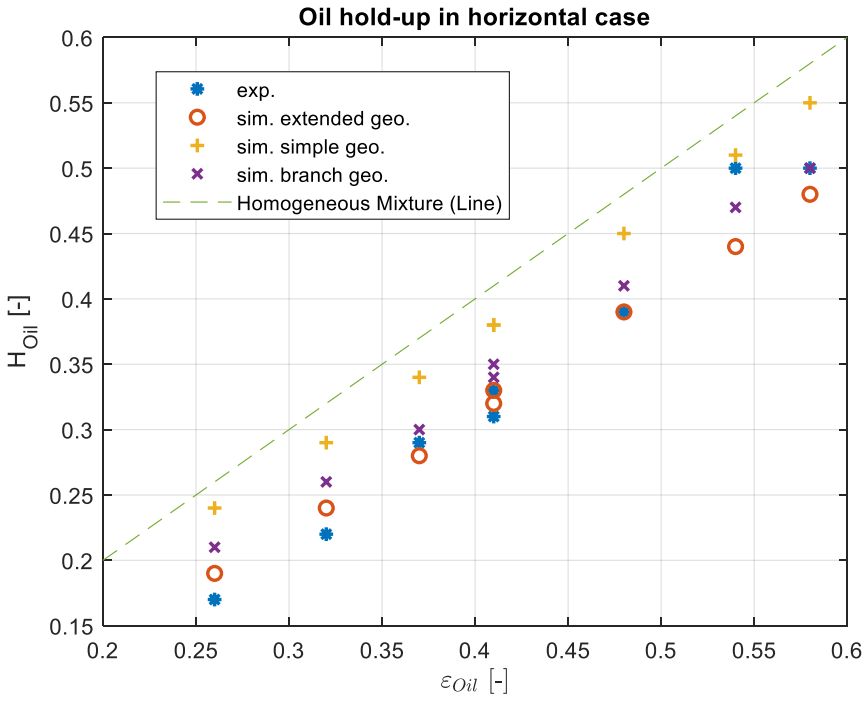

Figure 6 Plot of oil hold-up estimation in the experiment and simulated geometries for the horizontal case.

Table 4 shows the corresponding mean relative deviation (MRD) and mean relative absolute deviation (MARD) between the simulations and the experiments for the horizontal case. In cases of simple and branch geometry, MRD and MARD are quantitatively similar. While there is roughly a 5% difference between MRD and MARD for the case of extended geometry. This could be explained more visually in Figure 6 taking the red and blue dots corresponding to simulation results of the extended geometry and the experimental ones. For low values of the oil input fraction, the red dots are above the blue dots, reversely, for high values of the oil input fraction the red dots are below the blue dots. In other words, there is an overestimation and underestimation of hold-up captured by simulation of the extended geometry in comparison with the experimental hold-up depending on the value of oil input fraction.

Table 4 Corresponding Mean Relative Deviation (MRD) and Mean Relative Absolute Deviation (MARD)

	MRD	**MARD**
Sim. Extended Geo.	1%	6%
Sim. Simple Geo.	19%	19%
Sim. Branch Geo.	8%	9%

The maximum deviation of hold-up in the case of the 'extended' geometry is recorded at around 13%. Overall, out of the three mentioned geometrical cases, the 'extended' geometry provides the closest prediction of hold-up out of the three mentioned geometrical structures. For further calibration of the 'inclined' case, only the extended geometry is considered.

4.2. MESH DEPENDENCY

This subsection aims to provide a mesh dependency study. It is essential to make sure the mesh is sufficiently fine in terms of the number of cells so that the final results do not depend on the mesh level. This is a common approach in any sort of computational fluid dynamics problem.

Table 5 represents the details of the mesh dependency check for the worst-case 'D4' in terms of relative deviation. For this thesis work, 3 levels of mesh grid are tested. Levels 1 and 2 correspond to the coarse and medium respectively with 535 K and 858 K elements. The mesh is further adapted at the interface of the phases. The result corresponds to level 3 with a 2.8 M number of elements. However, it turns out that adapting the mesh does not make a huge difference in the accuracy of results. In this regard, refining the mesh up to level 2 (858K number of elements) suffice for the rest of the simulations.

Table 5 Mesh dependency representation details for case D4

	$-\frac{dP}{dz}\Big\|_{f,exp}\left[\frac{Pa}{m}\right]$	$-\frac{dP}{dz}\Big\|_{f,sim}\left[\frac{Pa}{m}\right]$	Error	$H_{Oil,exp}$	$H_{Oil,sim}$	Error
Level 1: 535K	1346	1590	18.1%	0.351	0.364	3.5%
Level 2: 858K	1346	1527	13.4%	0.351	0.363	3.2%
Level 3: 2.8M adapted version	1346	1512.6	12.4%	0.351	0.355	1.0%

4.4. HOLD-UP ESTIMATION

In this subsection, the aim is to quantitatively compare the simulation and experimental results in terms of phase hold-up. Based on the fact that the experimental phase hold-up was captured by Franchi for only a small section at the ending part of the set-up, the simulation phase hold-up is estimated surface based at the outlet for the sake of comparison between simulation and experiments. This is simply because it is presumed that at some point within the 3m simulated tube, the flow regime reaches a fully developed state after which there would be no change in the field variables including the phase hold-up.

$$H_{sim} = \frac{Outlet\ area\ covered\ by\ phase}{Total\ outlet\ area} \tag{18}$$

To further investigate the computational model versus the simulation, one can define a term as the relative deviation of hold-up:

$$RD_H = \frac{H_{sim} - H_{exp}}{H_{exp}} * 100\ \% \tag{19}$$

Figure 2 sketches the distribution of RD_H along the tube length for 8 cases as specified in the legend bar. The reference location L = 0 corresponds to the flow entrance to the main tube right after the initial mixture of oil and water in the nozzle section. This figure indicates that phase hold-up develops in a way that its relative deviation with experimental results plateaus and reaches a 20% range of values at certain points (say 2.5 m). This statement is visually observed in the phase pattern snapshots in Figure 11.

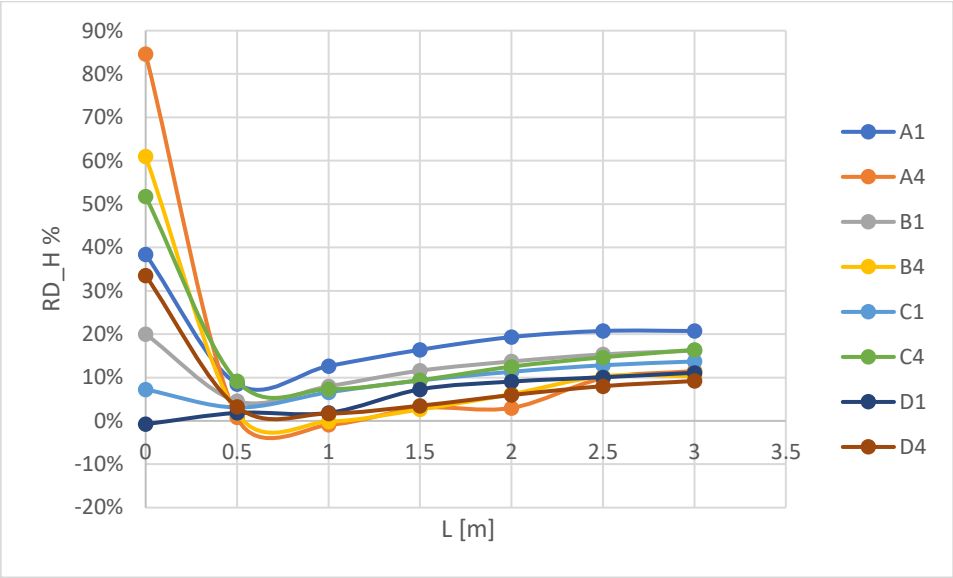

Figure 7 Plot of phase hold-up relative deviation along the tube length for 8 different inlet cases

Given the selected extended geometry and mesh, the simulation is set up for the inclined case. Figure 8 shows the trend of outlet oil hold up concerning oil flow rate fraction, setting k-epsilon and Transition SST turbulence model. For low values of input oil flow rate fraction, both models accurately predict the phase hold-up. While for high values of input oil flow rate fraction, the Transition SST Turbulence model results in higher accuracy. Figure 8 represents the parity plot of hold-up simulation vs. experiment. Table 6 shows the turbulence methods phase hold-up prediction preferences. Both k-eps and Trans SST seem to have the same MRD and MARD of 4%.

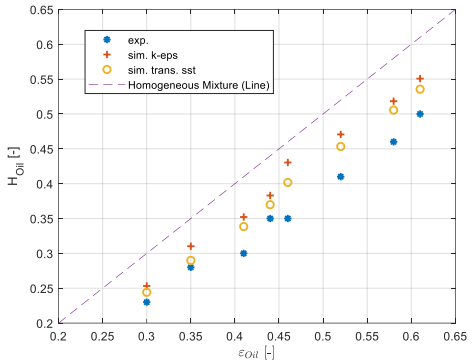

(a) Normal plot (hold-up vs oil inlet flow rate fraction)

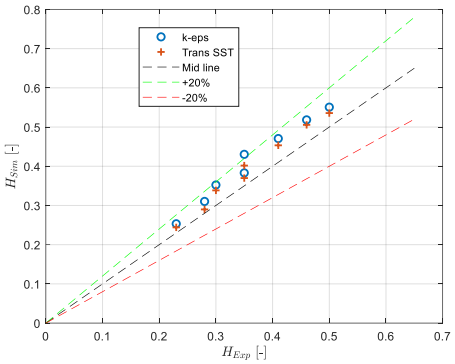

(b) Parity plot (simulation vs. experiment)

Figure 8 Plot of holdup estimation corresponding to different turbulence models (k-eps, and Transition SST)

Table 6 Prediction preference of the turbulence method based on hold-up

	MRD [%]	MARD [%]
K-eps	4	4
Trans SST	4	4

4.5. PRESSURE DROP ESTIMATION

This subsection aims to quantitatively compare the simulation and experimental results in terms of pressure drop. The average value of static pressure is calculated for every 0.5 m along the simulated tube. E.g. taking case A1, Figure 9 shows the values of static pressure and the corresponding linear trend line with a root mean squared value of 99.9%. Accordingly, the slope would represent the distributed pressure drop. The same is applied to all the other inlet cases.

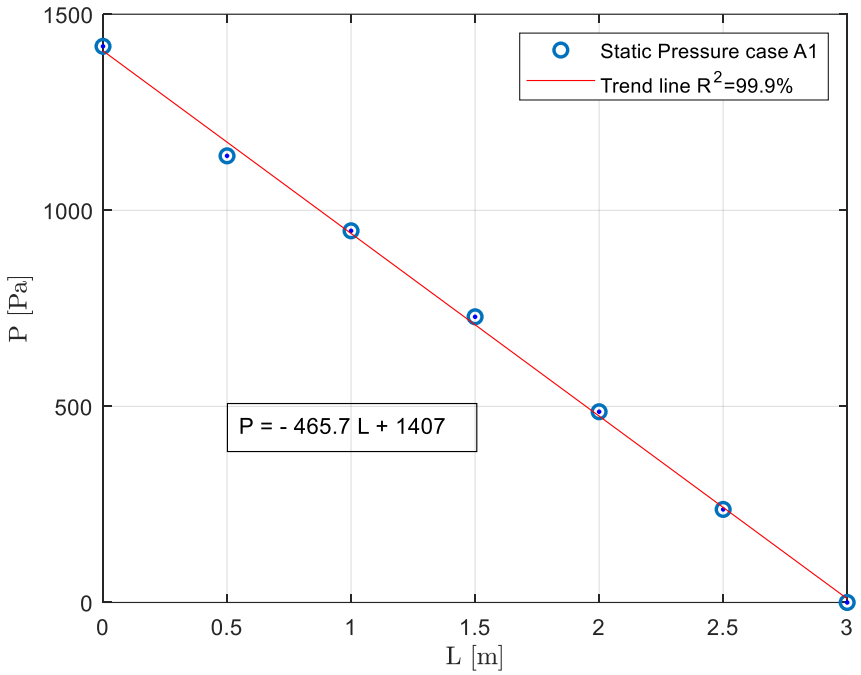

Figure 9 Plot of static pressure vs. tube length and the corresponding linear trend, the slope represents the distributed pressure drop (sample case 'A1')

Figure 10 represents the parity plot of frictional pressure drop derived out of the simulations vs. experiments for the k-eps and Trans SST model. All the predicted pressure drop values lie within the range of -20 % and +20 % deviation from the experiment.

Table 6 represents the turbulence method pressure drop prediction preferences. K-epsilon seems to be slightly more precise (by a relative margin of 1%) than TRANS SST in the prediction of the experiment with an MRD of -4 % and a MARD of 7 %.

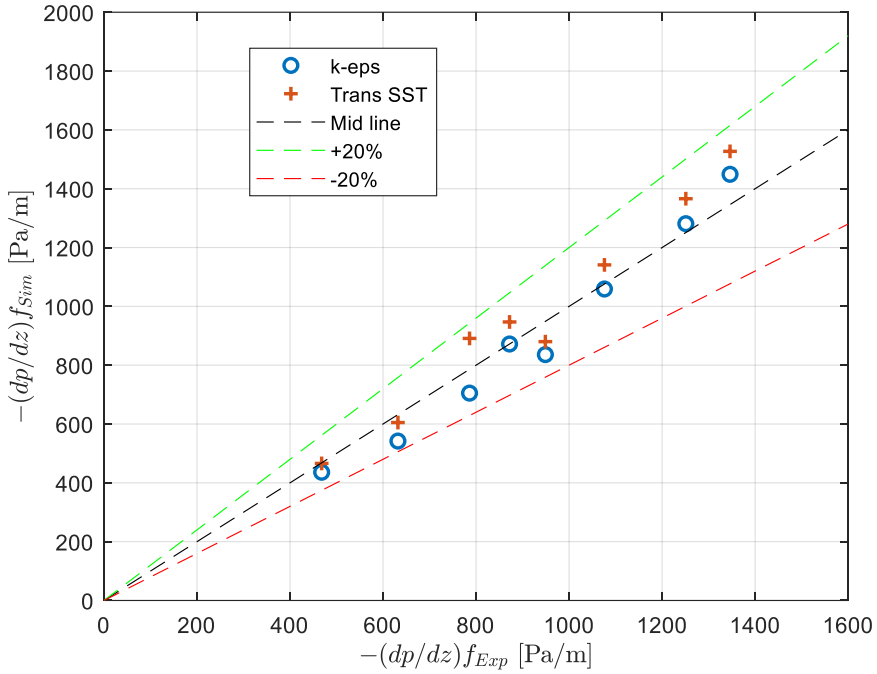

Figure 10 Parity plot of frictional pressure drop. Simulation vs. Experiment

Table 7 Prediction preference of the turbulence method based on frictional pressure drop

	MRD [%]	MARD [%]
K-eps	-4	7
Trans SST	5	8

4.3. FLOW PATTERN

This subsection aims to provide a graphical representation of the simulated regime of the oil-water core annular multiphase flow inside the set-up. Figure 11 demonstrates some snapshots of cross-sectional phase distribution at certain locations along the tube for each specific case. At the reference location, the hold-up is the same for all cases. Moving from the reference location, towards the outlet, the shape of the core column floats up whilst stretching circumferentially. From the physical point of view, this phenomenon occurs mainly due to the density difference of the phases as oil holds a lower density than water.

Taking cases ‘A1’, ‘B1’, ‘C1’, and ‘D1’, the water inlet flow rate is fixed, and oil superficial velocity rises respectively. Quantitatively, oil hold-up in case ‘D1’ is the highest of the four. The same is true for cases ‘A4’, ‘B4’, ‘C4’, and ‘D4’. In addition, moving from case ‘A’ to ‘B’, ‘C’, and ‘D’ successively, the shape of the oil core develops more towards completing a half-cylinder inside the tube. Hence the degree of eccentricity for the core column drops. Vice versa, as the water inlet flow rate escalates, fixing the oil inlet flow rate (e.g., take ‘A1’ and ‘A4’), oil hold-up drops, and the core column shrinks towards the center.

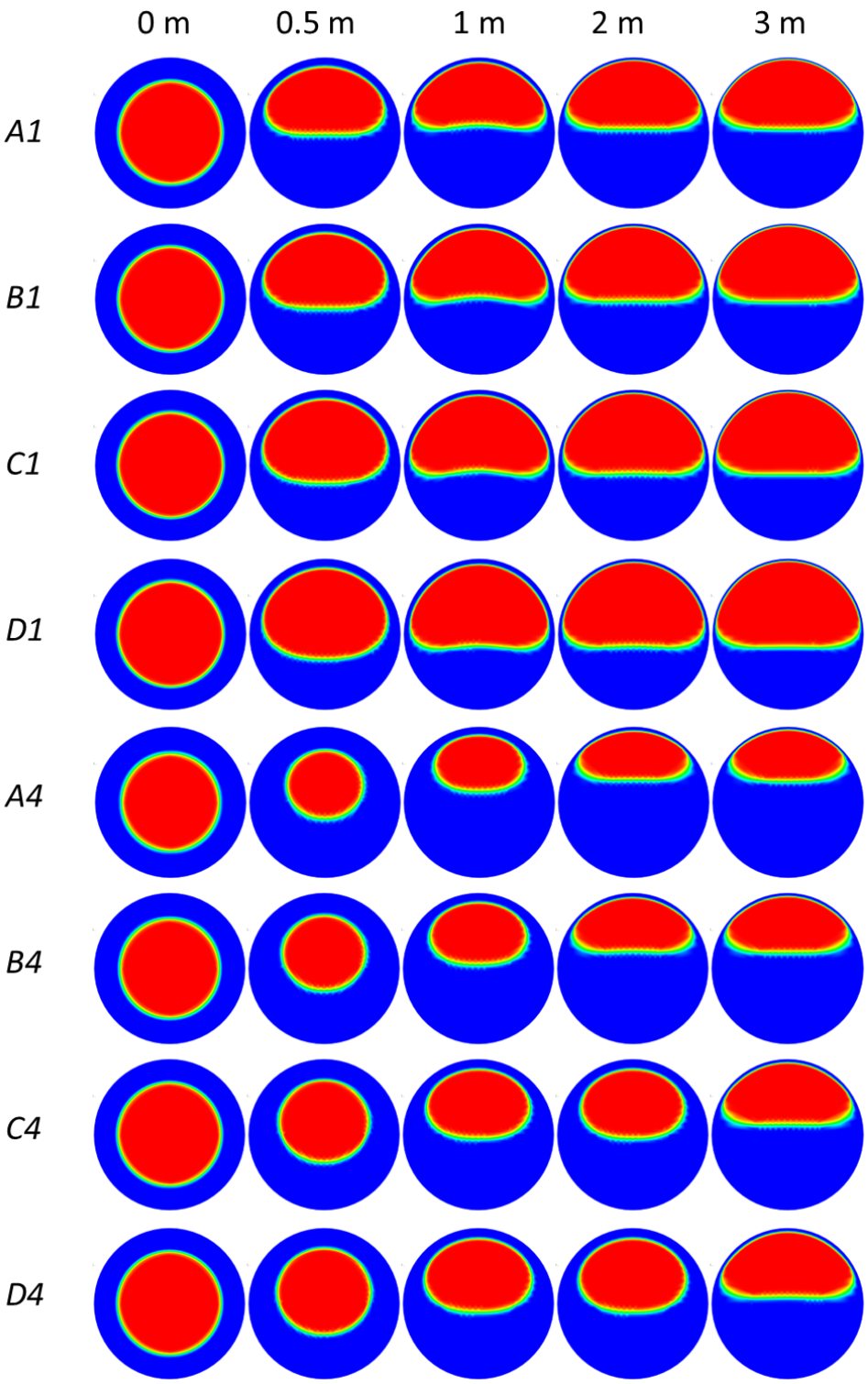

Figure 11 Snapshots of cross-sectional contours of phase hold-up along the tube

sample case D4 in (a) Simulation and (b) Experiment. In the simulation, the core goes through a smooth transfer from the center to the middle top section along the length of the tube. This transfer seems to occur also in the experiment. However, snapshots of the oil-water core annular flow regime in the experiment exhibit some waviness with random droplet detachments from the oil core. This behavior is not

captured in the simulation probably due to the selection of k-eps and Trans SST turbulency models in ANSYS Fluent. To capture accurate and reliable predictions in this regard, it is recommended to conduct Large Eddy Simulations instead of Reynolds Average Navier Stokes for the turbulency models.

(a) Simulation (the flow enters from the top right and leaves from the bottom left)

(b) Experiment [1]

Figure 12 Snapshot of longitude contour of phase hold-up along the tube for sample case D4

4.6. VELOCITY FIELD

In this subsection, the aim is to observe how the velocity field of the mixture develops along the tube. Presuming sample case D4, Figure 13 (a) and (c) respectively represents the cross-sectional and longitude contours of the velocity field. Figure 13 (b) sketches the center line velocity along the inclined tube. Right after the initial mixture of the phases in the nozzle, the flow enters the tube in a turbulent condition. This is observed both graphically in the snapshot contours and quantitively in the figure of centerline velocity. Approximately after a portion meter length of the tube, the flow starts to stabilize and reach a developed condition where the velocity field stays fixed along the tube.

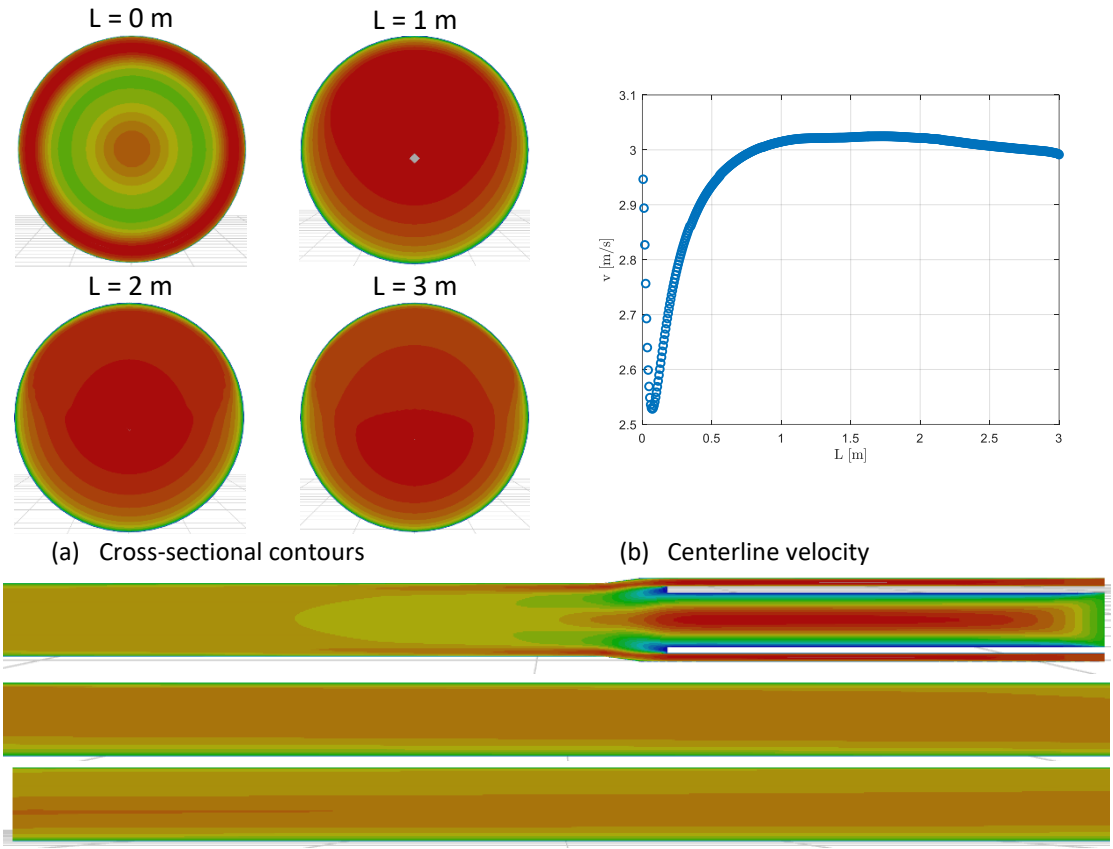

(a) Cross-sectional contours (b) Centerline velocity

(c) Longitude contours (the flow enters from top right and leaves from bottom leftS)

Figure 13 Velocity field for sample case D4

4.6. FRICTION FACTOR

The wall shear stress by definition can be expressed as

$$\tau_s = \frac{1}{2} f \rho u^2 \tag{20}$$

Where *f* is the so-called fanning friction factor, a dimensionless term used mainly for the calculation of fluid flows in pipes as adopted from the Moody diagram in 1944 [4]. Therefore one may derive and calculate the fanning friction factor directly from the original Eq.20, given the local wall shear stress out of the simulations in ANSYS Fluent.

$$f^* = 2\frac{\tau_s}{\rho_b J^2} \tag{21}$$

Where J is the mixture of superficial velocity and $\boldsymbol{\rho_b}$ is the bulk mixture density $\boldsymbol{\rho_b} = \boldsymbol{\varepsilon_O} * \boldsymbol{\rho_O} + (\mathbf{1} - \boldsymbol{\varepsilon_O}) * \boldsymbol{\rho_W}$. On the other hand, one might argue that the friction factor and wall shear stress associates only with the properties of water, not the bulk mixture since oil is in the core having no contact with the wall. In other words, in this regime of oil-water core annular flow, it is only water wetting the wall. In this regard, one might define the friction factor as follows:

$$f_w = 2\frac{\tau_s}{\rho_W u_w^2} \tag{22}$$

To assess which definition would make more sense here, suppose the trend of both friction factors as sketched in Figure 14 concerning the Reynolds number of the mixture, where:

$$Re_{mix} = \frac{\rho_b JD}{\mu_w} \tag{23}$$

It is common in the literature to express friction factor in the horizontal tube as a fitted power-law formulation:

$$f = \frac{C}{Re^n} \tag{24}$$

Whereas in the case of Blasius formulation $\boldsymbol{C = 0.316}$ and $\boldsymbol{n = 0.25}$. In the case of inclined pipes, a buoyancy term 'B' is usually added to the previous formulation [1]:

$$f = \frac{C}{Re^n} + B \tag{25}$$

Figure 14 plots the fanning friction factor versus the Reynolds number. The graph presents the trend for $\boldsymbol{f^*}$ and $\boldsymbol{f_w}$ togather with the Blasius correction formulation [5] representing a single phase fully turbulent flow of water in a tube of no roughness.

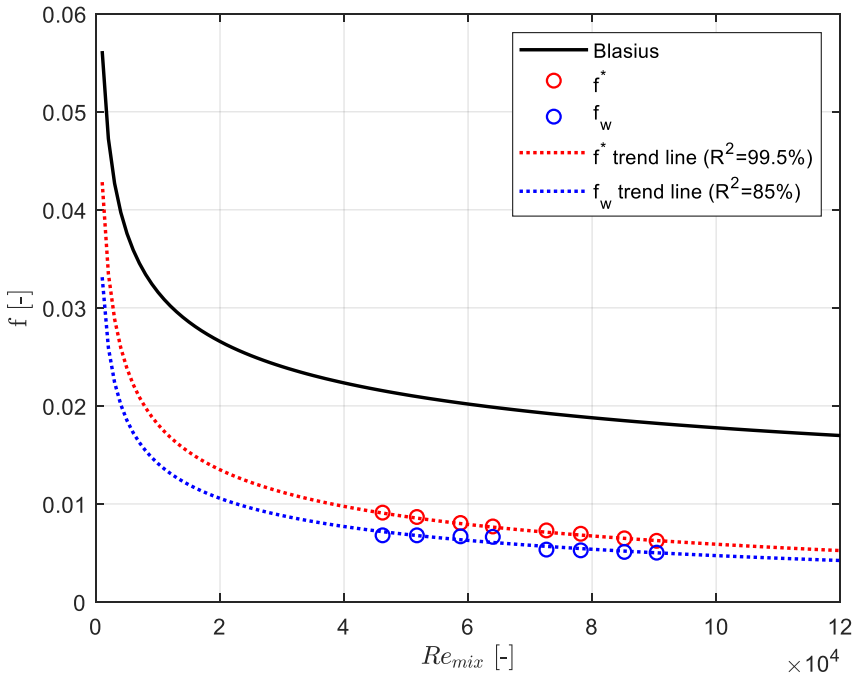

Figure 14 Plot of fanning friction factor versus the Reynolds number of the mixture

Table 8 presents the coefficients of the trend lines fitted over the mentioned fanning friction factors as well as the root mean squared of the fitting lines. Consequently $\boldsymbol{f}^*$ achieves a more accurate trend line with a root mean squared of 99.5 %.

Table 8 Coefficients of the fitted trend lines for fanning friction factor

	C	n	B	R^2
Blasius	0.316	0.25	----	----
f^*	0.4058	- 0.3065	- 0.006016	99.5 %
f_w	0.312	- 0.3065	- 0.004425	85 %

This qualitative analysis of the friction factor indicates that the oil-water core annular stream flows approximately with four times less friction in comparison to the single-phase stream of water in a tube of no roughness. This is simply due to the lubricating effect of water.

4.7. SUMMARY & DISCUSSION

Overall, three different geometries were investigated for simulation of oil-water core annular flow in the horizontal case. The 'simple', the 'branch', and the 'extended' version. Based on qualitative comparisons between simulation and experiment, the extended geometry, as well as the branch, seemed to provide almost equally high accurate results in terms of hold-up and frictional pressure drop. It was required to make an unstructured mesh for the branch geometry. Subsequently, this leads to an increase in the number of elements and thus higher computational cost. Therefore, it was more convenient to conduct the simulations in the extended version of the geometry.

Since the simulation geometry is only 3m as opposed to the actual 10 m experimental set-up, one might argue that it would be wrong to set the outlet BC as a pressure outlet while in the real case the pressure at L=3m is not equal to the environment. This is a valid and rational argument yet it is tested by setting a non-zero Dirichlet Outlet Pressure BC. After testing, it turns out that this change would only elevate the static pressure of the whole system while the pressure drop per unit length of the tube remains constant. In other words, no matter the total length of the simulated geometry, the frictional pressure drop per unit length of the tube stays the same.

5

Concluding Remarks

The present thesis aimed to contribute to the computational observation and validation of the oil-water core annular multiphase flow. To optimize the computational cost, a realistic geometry was modeled based on the experimental set-up in the Multiphase Thermal Fluid Dynamics Laboratory at the Energy Department of Polytechnic di Milano. The computational set-up was created in ANSYS Fluent 2020 R2. The volume of Fluid (VOF) and K-eps/Transition SST respectively were selected as the multiphase flow and turbulency models. Phase hold-up and frictional pressure drop are taken as system response quantities to assess the accuracy and reliability of the computational model. The simulation results replicate the experiments, yet some controversial arguments exist.

5.1. CONCLUSIONS

Franchi measured the phase hold-up at the end of the 10-meter-long set-up. He measured phase hold-up using the *quick closing* valves method in which 2 separate valves were installed on the sides of a known-volume pipe section at the ending part of the set-up. Switching off the pumps simultaneously and letting the mixture sediment, the phase hold-up would be known, removing the water and measuring its volume [1].

On the other hand, as mentioned previously, to reduce the computational cost, the length of the tube in simulations would be set to only 3m long. This geometrical inconsistency in the length of the actual set-up and simulation geometry indicates that it might not make sense to take phase hold-up as a system response quantity (SRQ) to be measured for validation purposes. This is simply because phase hold-up

might vary if the actual 10 m geometry was adopted. However, one could argue as long as the flow reaches its fully developed condition, the downstream regime of the flow stays the same no matter the length of the geometry! Yet this controversial hypothesis requires further investigation.

5.2. RECOMMENDATIONS FOR FUTURE WORK

RANS models such as K-eps and Transition SST predict the phase hold-up and distributed pressure drop with sufficient accuracy. However, these two RANS models predict a relatively smooth regime of the oil-water core annular multiphase flow. While in reality, as observed from the experimental photos, the regime of the multiphase flow contains particular waviness and oil droplet, detachments. These types of complexities in the flow stream require more accurate turbulency models e.g. Large Eddy Simulation (LES) or Detached Eddy Simulations (DES). These turbulency models have the potential to capture reliable and accurate results. However, the downside is that they normally entail a much higher computational cost and higher simulation complexity.

Bibliography

[1] Franchi, R. A. (2021). Effect of the down-slope on the structure and the pressure losses of an oil-water stream, Master's thesis, Politecnico di Milano

[2] S. Bollati (2014). Misure di cadenti di flussi acqua-olio in tubi orizzontali con brusco restringimento di sezione, Master's thesis, Politecnico di Milano

[3] Ghosh, S., Mandal, T. K., Das, G., & Das, P. K. (2009). Review of oil-water core annular flow. Renewable and Sustainable Energy Reviews, 13(8), 1957-1965.

[4] White, F. M. (1999). Fluid mechanics. Boston, Mass: WCB/McGraw-Hill.

[5] Blasius, H. (1913). Das aehnlichkeitsgesetz bei reibungsvorgängen in flüssigkeiten. In Mitteilungen über Forschungsarbeiten auf dem Gebiete des Ingenieurwesens (pp. 1-41). Springer, Berlin, Heidelberg.

[6] Gupta, V. K., Khan, M., & Punekar, H. (2015, December). Development and application of interfacial anti-diffusion and poor mesh numeric treatments for free surface flows. In 2015 IEEE 22nd International Conference on High Performance Computing Workshops (pp. 12-18). IEEE.

[7] ANSYS, Inc. (2016) ANSYS Fluent User's Guide, Release 17.2.

[8] Halpern, L., & Schatzman, M. (1989). Artificial boundary conditions for incompressible viscous flows. SIAM Journal on Mathematical Analysis, 20(2), 308-353.

[9] Son, G. (2001). A numerical method for incompressible two-phase flows with open or periodic boundaries. Numerical Heat Transfer: Part B: Fundamentals, 39(1), 45-60.

[10] Sohankar, A., Norberg, C., & Davidson, L. (1998). Low-Reynolds-number flow around a square cylinder at incidence: study of blockage, onset of vortex shedding and outlet boundary condition. *International journal for numerical methods in fluids*, *26*(1), 39-56.

[11] Papanastasiou, T. C., Malamataris, N., & Ellwood, K. (1992). A new outflow boundary condition. *International journal for numerical methods in fluids*, *14*(5), 587-608.

[12] Ol'Shanskii, M. A., & Staroverov, V. M. (2000). On simulation of outflow boundary conditions in finite difference calculations for incompressible fluid. *International Journal for Numerical Methods in Fluids*, *33*(4), 499-534.

[13] Lou, Q., Guo, Z., & Shi, B. (2013). Evaluation of outflow boundary conditions for two-phase lattice Boltzmann equation. Physical review E, 87(6), 063301.

[14] Leone Jr, J. M. (1990). Open boundary condition symposium benchmark solution: stratified flow over a backward-facing step. *International Journal for Numerical Methods in Fluids*, *11*(7), 969-984.

[15] Jin, G., & Braza, M. (1993). A nonreflecting outlet boundary condition for incompressible unsteady Navier-Stokes calculations. *Journal of computational physics*, *107*(2), 239-253.

[16] Gao, H., Gu, H. Y., & Guo, L. J. (2003). Numerical study of stratified oil–water two-phase turbulent flow in a horizontal tube. *International Journal of Heat and Mass Transfer*, *46*(4), 749-754.

[17] Dong, S. (2014). An outflow boundary condition and algorithm for incompressible two-phase flows with phase field approach. *Journal of Computational Physics*, *266*, 47-73.

[18] Angeli, P., & Hewitt, G. F. (2000). Flow structure in horizontal oil–water flow. *International journal of multiphase flow*, *26*(7), 1117-1140.

[19] Bochio, G., Cely, M. M., Teixeira, A. F., & Rodriguez, O. M. (2021). Experimental and numerical study of stratified viscous oil–water flow. *AIChE Journal*, *67*(6), e17239.

[20] Dewangan, S. K., Senapati, S. K., & Deshmukh, V. (2020). CFD investigation of parameters affecting oil-water stratified flow in a channel. *International Journal of Mathematical, Engineering and Management Sciences*, *5*(4), 602.

[21] Santos, D. S., Faia, P. M., Garcia, F. A. P., & Rasteiro, M. G. (2019). Oil/water stratified flow in a horizontal pipe: simulated and experimental studies using EIT. *Journal of Petroleum Science and Engineering*, *174*, 1179-1193.

[22] Li, Y., Choi, J. I., Choic, Y., & Kim, J. (2017). A simple and efficient outflow boundary condition for the incompressible Navier–Stokes equations. *Engineering Applications of Computational Fluid Mechanics*, *11*(1), 69-85.

[23] Halpern, L. (1986). Artificial boundary conditions for the linear advection diffusion equation. Mathematics of computation, 46(174), 425-438.

[24] Dehkordi, P. B., Colombo, L. P. M., Guilizzoni, M., & Sotgia, G. (2017). CFD simulation with experimental validation of oil-water core-annular flows through Venturi and Nozzle flow meters. Journal of Petroleum science and Engineering, 149, 540-552.

[25] Colombo, L. P., Guilizzoni, M., Sotgia, G., Dehkordi, P. B., & Lucchini, A. (2017, November). Water holdup estimation from pressure drop measurements in oil-water two-phase flows by means of the two-fluid model. In *Journal of Physics: Conference Series* (Vol. 923, No. 1, p. 012012). IOP Publishing.

List of Figures

List of Tables

Scuola di ingegneria industriale e dell'informazione
Polytechnic of Milan

Piazza Leonardo da Vinci, 32
20133 Milano
P.IVA 04376620151
C.F. 80057930150

https://www.polimi.it

Dipartimento di Energia

Campus Bovisa - Via Lambruschini, 4a - 20156 Milano
Tel. +39 02 2399 3801 – Fax +39 02 2399 3913
PEC pecenergia(at)cert.polimi.it
P.IVA: 04376620151
C.F. 80057930150

https://www.energia.polimi.it

July 2022